OPEN ACCESS

Original research

# Plaque morphology in acute symptomatic intracranial atherosclerotic disease

Thomas W Leung ,[1] Li Wang,[1] Xinying Zou,[2] Yannie Soo ,[1] Yuehua Pu,[2] Hing Lung Ip,[1] Anne Chan,[1] Lisa Wing Chi Au,[1] Florence Fan,[1] Sze Ho Ma,[1] Bonaventure Ip ,[1] Karen Ma,[1] Alexander Yuk-lun Lau ,[1] Howan Leung,[1] Kwok Fai Hui,[3] Richard Li,[4] Siu Hung Li,[5] Michael Fu,[6] Wing Chi Fong,[7] Jia Liu,[8] Vincent Mok,[1] Ka Sing Lawrence Wong,[1] Zhongrong Miao,[9] Ning Ma ,[9] Simon C H Yu ,[10] Xinyi Leng [1]

► Additional material is published online only. To view, please visit the journal online (http://dx.doi.org/10.1136/jnnp-2020-325027).

For numbered affiliations see end of article.

**Correspondence to**
Dr Xinyi Leng, Departments of Medicine and Therapeutics, The Chinese University of Hong Kong, Prince of Wales Hospital, Hong Kong SAR, China; xinyi_leng@cuhk.edu.hk and Dr Simon C H Yu, Department of Imaging and Interventional Radiology, The Chinese University of Hong Kong, Prince of Wales Hospital, Hong Kong SAR, China; simonyu@cuhk.edu.hk

Received 3 September 2020
Revised 19 October 2020
Accepted 6 November 2020
Published Online First 25 November 2020

Check for updates



**To cite:** Leung TW, Wang L, Zou X, *et al*. *J Neurol Neurosurg Psychiatry* 2021;**92**:370–376.

## ABSTRACT

**Background** Intracranial atherosclerotic disease (ICAD) is globally a major ischaemic stroke subtype with high recurrence. Understanding the morphology of symptomatic ICAD plaques, largely unknown by far, may help identify vulnerable lesions prone to relapse.

**Methods** We prospectively recruited patients with acute ischaemic stroke or transient ischaemic attack attributed to high-grade ICAD (60%–99% stenosis). Plaque morphological parameters were assessed in three-dimensional rotational angiography, including surface contour, luminal stenosis, plaque length/thickness, upstream shoulder angulation, axial/longitudinal plaque distribution and presence of adjoining branch atheromatous disease (BAD). We compared morphological features of smooth, irregular and ulcerative plaques and correlated them with cerebral ischaemic lesion load downstream in MRI.

**Results** Among 180 recruited patients (median age=60 years; 63.3% male; median stenosis=75%), plaque contour was smooth (51 (28.3%)), irregular (101 (56.1%)) or ulcerative (28 (15.6%)). Surface ulcers were mostly at proximal (46.4%) and middle one-third (35.7%) of the lesions. Most (84.4%) plaques were eccentric, and half had their maximum thickness over the distal end. Ulcerative lesions were thicker (medians 1.6 vs 1.3 mm; p=0.003), had steeper upstream shoulder angulation (56.2° vs 31.0°; p<0.001) and more adjoining BAD (83.3% vs 57.0%; p=0.033) than non-ulcerative plaques. Ulcerative plaques were significantly associated with coexisting acute and chronic infarcts downstream (35.7% vs 12.5%; adjusted OR 4.29, 95% CI 1.65 to 11.14, p=0.003). Sensitivity analyses in patients with anterior-circulation ICAD lesions showed similar results in the associations between the plaque types and infarct load.

**Conclusions** Ulcerative intracranial atherosclerotic plaques were associated with vulnerable morphological features and had a higher cumulative infarct load downstream.

## INTRODUCTION

Intracranial atherosclerotic disease (ICAD) is a major ischaemic stroke subtype of high recurrence.[1] In the Stenting and Aggressive Medical Management for Preventing Recurrent Stroke in Intracranial Stenosis (SAMMPRIS) trial, risk of recurrent stroke or death for patients with high-grade ICAD was 12.6% in the first year despite optimal medical treatment.[2] In the Chinese Intracranial Atherosclerosis study, a population-based cohort, 15% of ICAD patients with multiple vascular risk factors had stroke recurrence over 1 year.[3]

In contrast to coronary/carotid artery plaques where established imaging features might predict a myocardial or cerebral ischaemic event,[4–9] the morphology of ICAD lesions immediately after or portending a stroke was largely unknown. The sole parameter forecasting stroke relapse in symptomatic ICAD had been 'luminal stenosis' which, however, might imply distal perfusion deficit alone but would not account for stroke mechanisms like artery-to-artery thromboembolism, lacunar syndrome from junctional atheroma or branch hypoperfusion.[10 11] Of note, luminal narrowing in a third of ICAD lesions was only moderate at stroke onset, suggesting that factors beyond stenotic severity might also govern the stroke risks in patients with ICAD.

Therefore, a study on plaque morphology in acute symptomatic ICAD might improve our understanding of stroke occurrence/recurrence and inform treatment strategy.[5 12 13] In this study, we assessed ICAD plaque morphology by three-dimensional rotational angiography (3DRA), a catheter-based technique that enabled angioarchitecture evaluation from a near-infinite number of planes and could reveal plaque morphology and further subordinate branch/perforator patency in a superior spatial resolution compared with conventional digital subtraction angiography.[14 15] We compared morphological features of plaques with smooth, irregular and ulcerative contour and correlated the plaque morphological features with downstream cerebral ischaemic lesion load in MRI.

## MATERIALS AND METHODS

### Study design and subjects

This was a prospective, investigator-initiated multicentre-referral study. We recruited adult patients with acute ischaemic stroke or transient ischaemic attack (TIA) within 4 weeks of symptom onset, attributed to

high-grade ICAD (60%–99% stenosis) as confirmed in 3DRA. TIA was defined as a transient episode of neurological dysfunction caused by focal brain or retinal ischaemia that completely resolved within 24 hours. All patients underwent brain MRI. The stroke aetiology and relevance to ICAD were determined by neurologists, based on clinical syndrome, imaging features and concurrent cardiovascular risk factors. We excluded patients with probable non-atherosclerotic stenosis (eg, moyamoya disease, vasculitis or dissection), evidence of cardioembolism (eg, atrial fibrillation, valvular heart disease or myocardial infarction within 6 weeks), concurrent tandem >70% extracranial carotid or vertebral artery (VA) stenosis and contraindications to MRI and 3DRA. In this observational study, all patients received guideline-based treatment that evolved with emerging evidence. Of note, participants recruited before SAMMPRIS[16] received lifelong single antiplatelet treatment (aspirin), whereas those recruited after SAMMPRIS had short-term dual antiplatelets (aspirin plus clopidogrel) immediately after the index stroke, followed by lifelong aspirin. All patients received statins with a low-density lipoprotein target of <70 mg/dL (<1.8 mmol/L). Other goals of cardiovascular risk control, if applicable, included an HbA1c <6.5% and a systolic blood pressure <140 mm Hg.

## 3DRA and plaque morphology evaluation

In a neuroangiographic unit (Integris BN 3000 Neuro; Philips Medical Systems, Best, the Netherlands), we performed 3DRA within 4 weeks from the index stroke/TIA. A total volume of 20–25 mL Iopamiro300 was injected by an automated machine (2.0–2.5 mL/s) through a 4F endovascular catheter perching at the internal carotid artery (ICA)-C2 segment for distal ICA or middle cerebral artery (MCA)-M1 lesions, or at VA-V2 segment for vertebrobasilar lesions. 3DRA images were then reconstructed from 200 non-subtracted images captured during a 4 s 180° rotation of the C-arm around the lesion of interest with a maximal matrix of 512×512×512.[15]

One investigator (XL) with over 8 years' experience in interpreting and researching neurovascular images evaluated the culprit ICAD lesions in 3DRA in a Philips Allura Xper FD20/20 biplane neuro X-ray system (Koninklijke Philips N.V.). The plaque surface contour was classified into smooth, irregular (undulating plaque surface lining) or ulcerative subtype (figure 1A,B,C.[12 17] An ulcerative plaque was characterised by invagination of contrast beneath the endoluminal lining or have an upstream or downstream slope >90°.[17] In a plane that maximally displayed the luminal stenotic severity, we measured lesion length, per cent luminal stenosis, maximum plaque thickness, upstream plaque shoulder angulation and eccentricity index (figure 1). Whereas the assessment of surface contour, adjoining branch atheromatous disease (BAD) and axial plaque load distribution was based on 360° rotatory full-profile views of the target lesion. In patients with more than one spatially separated qualifying ICAD lesions, the lesion with the highest degree of luminal stenosis was assessed. Uncertainties in classification and measurement were resolved by consulting a senior neurologist and neurointerventionalist with 15 years' experience in neurointervention (TWL). We tested intrarater (XZ) and inter-rater (XZ and YP) reproducibility for the 3DRA measurements in 24 cases.

We measured percent luminal stenosis by Warfarin-Aspirin Symptomatic Intracranial Disease method.[18] Maximum plaque thickness was the height from the stenotic throat down to an extrapolated vessel wall drawn from both ends of the plaque, assuming natural tapering of the artery (figure 1D). Upstream plaque shoulder angulation was the angle between the proximal slope and the extrapolated vessel wall (figure 1E,F). We recorded the maximal plaque load over proximal, middle and distal one-thirds of the plaque in a longitudinal view (figure 1G,H,I). In a cross-sectional axial view, we assessed the plaque load over the superior, inferior, ventral and dorsal walls of MCA-M1 lesions, or the lateral, ventral and dorsal walls of basilar artery (BA) lesions. The circumferential plaque distribution was numerically expressed by eccentricity index, calculated as (maximum plaque thickness – minimum plaque thickness) / maximum plaque thickness. Plaques were eccentric if eccentricity index was ≥0.5 or concentric if <0.5 (figure 1J,K).[19]

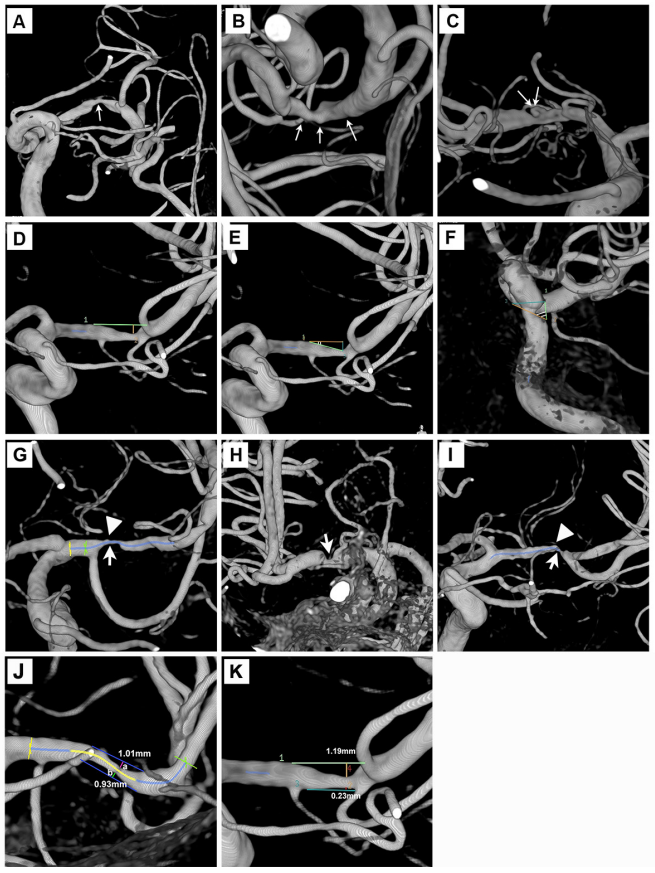


**Figure 1** Plaque morphology evaluation in three-dimensional rotational angiography. (A–C) Smooth, irregular or ulcerative plaques (thin white arrows). (D) Length and maximum plaque thickness of an MCA plaque. (E and F) Two upstream plaque shoulder angulations of 17° and 61°. (G–I) Maximum plaque burden (thick white arrows) at proximal, middle and distal 1/3 of the MCA lesions. High-grade adjoining branch atheromatous disease was noted in figure parts G and I (arrow heads). (J) A concentric plaque of eccentricity index 0.08. (K) An eccentric plaque of eccentricity index 0.81. MCA, middle cerebral artery.

Orifical narrowing of an adjacent branch/perforator >50% by a contiguous and morphologically inseparable plaque extending from the parent artery plaque defined 'adjoining BAD' (figure 1G,I).[20 21] For MCA lesions, we scrutinised lenticulostriate artery, anterior temporal artery and, occasionally, an early M2 branch emanating from the horizontal MCA segment. For BA lesions, we examined superior cerebellar artery and anterior inferior cerebellar artery.

## Cerebral ischaemic lesion assessment in MRI

Each participant received a brain MRI examination on a 1.5 tesla (Siemens Sonata, Germany) or 3.0 tesla MR scanner (Achieva 3.0T Philips, Netherlands), including axial T1-weighted and T2-weighted imaging, diffusion-weighted imaging (DWI), apparent diffusion coefficient mapping, T2 fluid-attenuated inversion recovery and time-of-flight MR angiography within a week from the index stroke/TIA. One investigator (XL) assessed

the cerebral ischaemic lesion load over the corresponding territory of a diseased intracranial artery. Evaluation of the MR images was at least 1 month after the 3DRA assessments, and the reviewer was blinded to the plaque morphological features except for the location of the culprit ICAD lesion. Acute infarct(s) was defined by high signal in DWI with low signal in apparent diffusion coefficient maps, and chronic infarct(s) was defined by high signal in T2 fluid-attenuated inversion recovery imaging and iso-intensity or high-intensity signal in apparent diffusion coefficient maps. We classified the infarct load in the corresponding territory as: (A) no infarct, (B) acute infarct(s) only or chronic infarct(s) only or (C) coexisting acute and chronic infarcts. We correlated cerebral ischaemic lesion load with clinical and 3DRA findings.

### Statistical analysis

We used IBM SPSS Statistics V.24.0 for statistical analyses. A two-sided $p<0.05$ was considered statistically significant. Continuous variables were expressed in medians (IQR) and categorical variables in numbers (percentages). Missing data were recorded. Kappa and intraclass correlation coefficients represented intrarater and inter-rater reproducibility for categorical and continuous variables. We used Wilcoxon rank-sum tests or Kruskal-Wallis tests for univariable comparisons of continuous variables and $\chi^2$ tests or Fisher's exact tests for categorical variables, in patients with different plaque types and in those with different infarct loads. Following a significant Kruskal-Wallis test, pairwise comparisons were conducted using the Dunn-Bonferroni post hoc method.

In univariable binary logistic regression analyses, we tested the associations of coexisting acute and chronic infarcts with demographics, clinical features and lab testing results, and culprit ICAD plaque types. In a multivariable binary logistic regression model, we tested for an independent relationship between plaque types and coexisting acute and chronic infarcts after adjusting for factors with $p<0.10$ in univariable logistic regression analyses. Crude and adjusted ORs with the 95% CIs were obtained. The logistic regression analyses were performed among all patients, and in patients with anterior circulation ICAD (sensitivity analysis).

### Data availability

Anonymised data that support the findings of this study are available from the corresponding author on reasonable request from qualified investigators.

## RESULTS

### Demographics and clinical features

From May 2007 to February 2018, we recruited 180 acute stroke patients with high-grade, symptomatic ICAD. The median age was 60 years (IQR 54–68), and 114 patients (63.3%) were male; 143 (79.4%), 123 (68.3%) and 64 (35.6%) patients, respectively, had a history of dyslipidaemia, hypertension and diabetes; 84 (46.7%) patients were smokers. The qualifying events were ischaemic strokes in 141 (78.3%) and TIA in 39 patients (21.7%). The median National Institutes of Health Stroke Scale on admission was 1 (IQR 1–3).

### ICAD plaque morphology

The median interval between stroke onset and 3DRA was 23 days (IQR 13–32). Table 1 summarises the morphological features of the 180 ICAD plaques. Among the 180 lesions, 132 were in MCA-M1, 26 in terminal ICA, 6 spanning across terminal ICA and MCA-M1, 14 in BA and 2 in VA. Intrarater (0.82–0.87) and inter-rater reproducibility (0.76–0.81) for the measurements were moderate to good in 24 cases.

The median luminal stenosis was 75% (IQR 71–84). Plaque contour was smooth (n=51; 28.3%), irregular (n=101; 56.1%) or ulcerative (n=28; 15.6%). There were 30 plaque surface ulcers identified in 28 ulcerative plaques. These surface ulcers indicative of fibrous cap rupture was found most frequently at the proximal (n=13; 46.4%) and middle one-third (n=10; 35.7%) of the plaques and relatively less at the distal end (n=7;

**Table 1** Morphological characteristics of all plaques and comparisons of different plaque types*

| Characteristics | Overall (N=180) | Plaque types | | | P value † | Smooth and irregular plaques (n=152) | P value ‡ |
|---|---|---|---|---|---|---|---|
| | | Smooth (n=51) | Irregular (n=101) | Ulcerative (n=28) | | | |
| Location of the qualifying ICAD lesions | | | | | 0.035 | | 0.048 |
| MCA-M1 | 132 (73.3) | 45 (88.2) | 72 (71.3) | 15 (53.6) | | 117 (77.0) | |
| Terminal ICA | 26 (14.4) | 4 (7.8) | 14 (13.9) | 8 (28.6) | | 18 (11.8) | |
| Across terminal ICA and proximal MCA | 6 (3.3) | 0 (0) | 4 (4.0) | 2 (7.1) | | 4 (2.6) | |
| VA-V4 or BA | 16 (8.9) | 2 (3.9) | 11 (10.9) | 3 (10.7) | | 13 (8.6) | |
| Arterial luminal stenosis, % | 75 (71–84) | 73 (70–79) | 78 (72–86) | 77 (72–81) | 0.027 | 75 (70–85) | 0.876 |
| Maximal plaque thickness, mm | 1.3 (1.2–1.6) | 1.3 (1.1–1.5) | 1.3 (1.2–1.6) | 1.6 (1.3–1.9) | 0.007 | 1.3 (1.1–1.6) | 0.003 |
| Plaque length, mm | 9.0 (6.9–11.6) | 7.0 (5.8–8.7) | 10.1 (8.0–13.2) | 9.0 (6.2–14.9) | <0.001 | 9.0 (6.9–11.6) | 0.873 |
| Eccentricity index | 0.87 (0.63–1.00) | 0.87 (0.68–1.00) | 0.83 (0.59–1.00) | 1.00 (0.80–1.00) | 0.164 | 0.85 (0.62–1.00) | 0.107 |
| Eccentric plaque | 152 (84.4) | 44 (86.3) | 83 (82.2) | 25 (89.3) | 0.599 | 127 (83.6) | 0.442 |
| Upstream plaque shoulder angulation,° | 33.4 (23.4–46.4) | 28.0 (21.1–43.6) | 33.1 (24.0–43.4) | 56.2 (30.6–94.2) | <0.001 | 31.0 (22.5–43.4) | <0.001 |
| Maximal stenosis distribution in the longitudinal axis of the lesion | | | | | 0.416 | | 0.321 |
| Proximal 1/3 of the lesion | 28 (15.6) | 6 (11.8) | 15 (14.9) | 7 (25.0) | | 21 (13.8) | |
| Middle 1/3 of the lesion | 63 (35.0) | 21 (41.2) | 33 (32.7) | 9 (32.1) | | 54 (35.5) | |
| Distal 1/3 of the lesion | 89 (49.4) | 24 (47.1) | 53 (52.5) | 12 (42.9) | | 77 (50.7) | |
| Adjoining branch atheromatous disease in cases with MCA-M1 or BA lesions | 88 (60.3) | 20 (43.5) | 53 (64.6) | 15 (83.3) | 0.007 | 73 (57.0) | 0.033 |

*Values are medians (IQR) or numbers (%); Kruskal-Wallis tests or Wilcoxon rank-sum tests were used for comparison of continuous variables and $\chi^2$ tests for categorical variables.
†P values for comparisons among smooth, irregular and ulcerative plaques.
‡P values for comparisons between ulcerative plaques and other plaques.
ICAD, intracranial atherosclerotic disease; MCA-M1, M1 middle cerebral artery; ICA, internal carotid artery; VA-V4, V4 vertebral artery; BA, basilar artery.

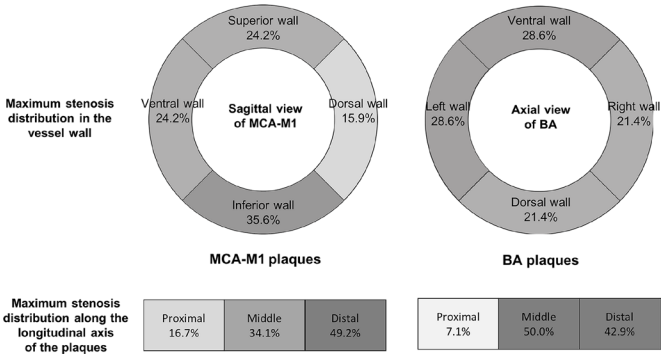


**Figure 2** Maximal stenosis distribution in 132 MCA-M1 plaques and 14 BA plaques by axial and longitudinal views. A darker colour indicates a higher frequency. Upper panel: frequencies of cases with the maximum plaque thickness located over the superior, inferior, ventral and dorsal walls of MCA-M1 (left); or over the ventral, dorsal and lateral walls of BA (right). Lower panel: frequencies of cases with the maximum plaque thickness located at the proximal, middle or distal one-third along the longitudinal axis of MCA-M1 (left) and BA (right) plaques. BA, basilar artery; MCA-M1, M1 middle cerebral artery.

25.0%). However, luminal plaque load, on the contrary, was skewed disproportionally to the distal end, in which a half of all plaques (n=89, 49.4%) had their maximum thickness (and hence maximum stenosis) recorded over the distal one-third (table 1 and figure 2).

The circumferential plaque distribution was eccentric in the vast majority of lesions (n=152; 84.4%). The median eccentricity index was 0.87 (IQR 0.63–1.00; table 1). Specifically, among the 132 MCA-M1 plaques, 47 lesions (35.6%) protruded maximally over the inferior vessel wall, 32 (24.2%) over the superior wall, 32 (24.2%) over the ventral wall and 21 (15.9%) over the dorsal wall. For the 14 BA plaques, seven lesions (50.0%) protruded maximally over the lateral walls, four (28.6%) over the ventral wall and three (21.4%) over the dorsal walls (figure 2). The median upstream plaque shoulder angulation was 33.4° (IQR 23.4°–46.4°; table 1).

Among 146 MCA-M1 or BA plaques, adjoining BAD was found in 88 lesions (60.3%; 80 MCA-M1 and 8 BA lesions), occluding the ostium of lenticulostriate artery (n=66), anterior temporal artery (n=29), an early M2 branch (n=7), anterior inferior cerebellar artery (n=7) and superior cerebellar artery (n=3). Some patients had adjoining BAD in more than one perforator/subordinate branch, and therefore, the number of small arteries with adjoining BAD exceeded the number of patients.

### Morphological differences of smooth/irregular/ulcerative plaques

Demographics, history of vascular risk factors or lab results did not differ between patients with or without ulcerative plaques; yet, patients harbouring ulcerative plaques had a higher fasting blood glucose level (medians 6.7 vs 5.7 mmol/L; p=0.047; online supplemental table 1). Overall, smooth, irregular and ulcerative plaques had different luminal stenosis (p=0.027); specifically, irregular plaques had significantly higher luminal stenosis than smooth plaques (medians 78% vs 73%; p=0.021), while there was no significant difference in luminal stenosis in other pairwise comparisons. Compared with non-ulcerative plaques, ulcerative plaques were thicker (medians 1.6 vs 1.3 mm; p=0.003), of a steeper upstream shoulder (medians 56.2° vs 31.0°; p<0.001) and were more frequently associated with adjoining BAD (83.3% vs 57.0%; p=0.033). Table 1 summarises the morphological characteristics of smooth, irregular and ulcerative plaques.

### Cerebral ischaemic lesion load and plaque types

The median interval between symptom onset and the MRI exam was 3 days (IQR 2–7). Of the infarct load in the corresponding territory, 26 patients (14.4%) had no infarct; 125 patients (69.4%) had acute infarct(s) only or chronic infarct(s) only; and 29 (16.1%) patients had coexisting acute and chronic infarcts.

Univariable and multivariable analyses for predictors of coexisting acute and chronic infarcts, in all patients and in patients with an anterior circulation lesion, are shown in tables 2 and 3 and online supplemental table 2 and 3. Comparing the three patterns of progressive infarct load, plaque morphology and clinical parameters (age, hypertension, diabetes, glycosylated haemoglobin and fasting blood glucose at the index stroke and plaque type) differed among the groups. Compared with the remaining patients, those with coexisting acute and chronic infarcts were more likely to have a history of hypertension (89.7% vs 64.2%; p=0.007) and ulcerative plaques (34.5% vs 11.9%; p=0.007) (table 2).

In univariable logistic regression analyses, history of hypertension (crude OR=4.83; 95% CI 1.40 to 16.68; p=0.013) and ulcerative plaques (crude OR vs otherwise=3.89; 95% CI 1.57 to 9.66; p=0.003) were significantly associated with coexisting acute and chronic infarcts in the corresponding territory (online supplemental table 3). In multivariable logistic regression analysis, patients harbouring ulcerative plaques were significantly more likely to have coexisting acute and chronic infarcts in the downstream vascular territory (35.7% vs 12.5%; crude OR=3.89, 95% CI 1.57 to 9.66, p=0.003; adjusted OR=4.29, 95% CI 1.65 to 11.14, p=0.003) than those with smooth or irregular plaques (table 3). Sensitivity analyses among patients with an anterior circulation lesion (n=164) showed similar results in univariable analyses (online supplemental table 2) and multivariable analyses (table 3). Figure 3 shows the MRI and 3DRA images of a patient with an ulcerative MCA-M1 plaque and coexisting acute and established infarcts in the corresponding cortical and subcortical regions, including the internal and posterior borderzones.

## DISCUSSION

In a prospective multicentre-referral study, we reported the morphology of acute symptomatic intracranial atherosclerotic plaques by 3DRA and correlated the plaque morphology with the downstream cerebral ischaemic lesion load. In summary, plaque contour was mostly irregular or ulcerative at the acute stage. Surface ulcers indicative of plaque rupture were mostly present over the upstream plaque region. By axial view, over 80% of the plaques were noted to be eccentric. By longitudinal view, the luminal plaque load was found disproportionally skewed to the distal end in half of the lesions. Compared with non-ulcerative plaques, ulcerative lesions had a significantly higher luminal plaque load, a steeper upstream shoulder and more adjoining BAD. Of note, ulcerative plaque was independently associated with more cumulative (ie, chronic plus acute) infarcts at the downstream regions.

As an imaging marker of fibrous cap rupture, plaque ulcer and the associated morphological features are potential clues to lesion vulnerability. In terms of atherosclerosis burden, a larger plaque volume may increase stroke risk by causing more severe luminal narrowing or perforator/branch jailing. Plaque rupture

**Table 2** Characteristics of patients with different infarct loads in the territory of the diseased intracranial artery of interest*

| Characteristics (n=180) | Infarct loads in the relevant territory: None (n=26) | Acute infarct(s) only or chronic infarct(s) only (n=125) | Coexisting acute and chronic infarcts (n=29) | P value † | P value‡ |
|---|---|---|---|---|---|
| Age, years | 55 (51–62) | 61 (55–69) | 62 (57–69) | 0.004 | 0.255 |
| Male | 19 (73.1) | 76 (60.8) | 19 (65.5) | 0.480 | 0.790 |
| Current smoker | 15 (57.7) | 52 (41.6) | 17 (58.6) | 0.121 | 0.159 |
| History of dyslipidaemia | 18 (69.2) | 100 (80.0) | 25 (86.2) | 0.287 | 0.325 |
| History of hypertension | 13 (50.0) | 84 (67.2) | 26 (89.7) | 0.006 | 0.007 |
| History of diabetes | 4 (15.4) | 46 (36.8) | 14 (48.3) | 0.034 | 0.118 |
| Systolic blood pressure, mm Hg | 152 (133–169) | 150 (136–165) | 159 (138–172) | 0.527 | 0.259 |
| Diastolic blood pressure, mm Hg | 85 (76–93) | 80 (70–90) | 83 (71–94) | 0.317 | 0.556 |
| Laboratory test results | | | | | |
| Glycosylated haemoglobin, % | 6.0 (5.3–6.4) | 6.2 (5.7–7.5) | 6.4 (5.9–7.5) | 0.030 | 0.353 |
| Fasting blood glucose, mmol/L | 5.1 (4.9–5.9) | 5.8 (5.1–7.3) | 6.4 (5.2–7.4) | 0.031 | 0.293 |
| Low-density lipoprotein, mmol/L | 3.3 (2.4–4.6) | 3.4 (2.7–4.1) | 3.3 (2.8–3.9) | 0.859 | 0.582 |
| High-density lipoprotein, mmol/L | 1.3 (1.0–1.5) | 1.1 (0.9–1.3) | 1.2 (0.9–1.5) | 0.091 | 0.277 |
| Triglycerides, mmol/L | 1.3 (0.9–1.6) | 1.5 (1.2–2.0) | 1.6 (1.2–2.1) | 0.143 | 0.890 |
| Location of the qualifying ICAD lesions | | | | 0.286 | 0.447 |
| MCA-M1 | 20 (76.9) | 91 (72.8) | 21 (72.4) | | |
| Terminal ICA | 1 (3.8) | 20 (16.0) | 5 (17.2) | | |
| Across terminal ICA and proximal MCA | 2 (7.7) | 2 (1.6) | 2 (6.9) | | |
| VA-V4 or BA | 3 (11.5) | 12 (9.6) | 1 (3.4) | | |
| Plaque types | | | | 0.032 | 0.007 |
| Smooth | 8 (30.8) | 38 (30.4) | 5 (17.2) | | |
| Irregular | 15 (57.7) | 72 (57.6) | 14 (48.3) | | |
| Ulcerative | 3 (11.5) | 15 (12.0) | 10 (34.5) | | |
| Arterial luminal stenosis, % | 78 (72–83) | 75 (71–85) | 75 (70–82) | 0.781 | 0.519 |

*Values are medians (IQR) or numbers (%); Kruskal-Wallis tests or Wilcoxon rank-sum tests were used for comparison of continuous variables and $\chi^2$ tests for categorical variables.
†P values for comparisons among the three groups.
‡P values for comparisons between patients with coexisting acute and chronic infarcts in the relevant territory and other patients.
ICAD, intracranial atherosclerotic disease; MCA-M1, M1 middle cerebral artery; ICA, internal carotid artery; VA-V4, V4 vertebral artery; BA, basilar artery.

risk may escalate over a steeper eccentric upstream shoulder that bears the brunt of the inflow accelerated jets. The high wall shear stress at the upstream zone could then lead to plaque ulceration followed by repetitive thromboembolisation.[22] This pathogenic mechanism might explain why most plaque ulcers were found at the proximal stenotic throats where flow jets and shear stress were maximal and, concordantly, the presence of more infarcts downstream. In coronary and carotid vasculature, surface irregularity and ulcers were also associated with enhanced wall shear stress at the upstream zone of the plaques.[23 24] These adverse geometry-related haemodynamic features may also portend an unfavourable clinical outcome. In a CT angiography-based computational fluid dynamic model, we revealed more stroke recurrences in symptomatic ICAD patients with increased flow jet and focal wall shear stress on the index high-grade stenoses.[22] The higher cumulative infarction downstream of ulcerative plaques might suggest repetitive artery-to-artery thromboembolism.[25] This observation might explain the efficacy of dual antiplatelet regimen during acute stage of ICAD[26 27] and a potential therapeutic application of blood flow augmentation in clearing the stranded emboli at the watershed regions.[28]

Basal ganglia or brainstem lacunar syndrome had been common in ICAD patients with infarct topography resembling small vessel disease. However, confirmation of branch/perforator disease in vivo had not been feasible with conventional angiographic techniques.[29] With 3DRA, we revealed the frequent coexistence of adjoining BAD within the perforator-rich stenotic segments, constituting a competing stroke mechanism: parent artery atherosclerosis occluding branch/perforator.[25] In fact, understanding the spatial relationship between parent artery and branches/perforators might have further clinical implications. First, ostial involvement of branches/perforators might highlight the risk of branch jailing by 'snow-plow effect' during intracranial angioplasty/stenting. As perforator stroke frequently

**Table 3** Multivariable logistic regression analyses for independent predictors of the presence of coexisting acute and chronic infarcts in the territory of the diseased intracranial artery

| Characteristics | All patients (n=180) OR (95% CI) | P value | Patients with anterior circulation ICAD (n=164) OR (95% CI) | P value |
|---|---|---|---|---|
| History of hypertension | 5.27 (1.48 to 18.75) | 0.010 | 5.74 (1.60 to 20.65) | 0.007 |
| Plaque types | | | | |
| Smooth/irregular | 1.00 | | 1.00 | |
| Ulcerative | 4.29 (1.65 to 11.14) | 0.003 | 4.88 (1.80 to 13.22) | 0.002 |

ICAD, intracranial atherosclerotic disease.;

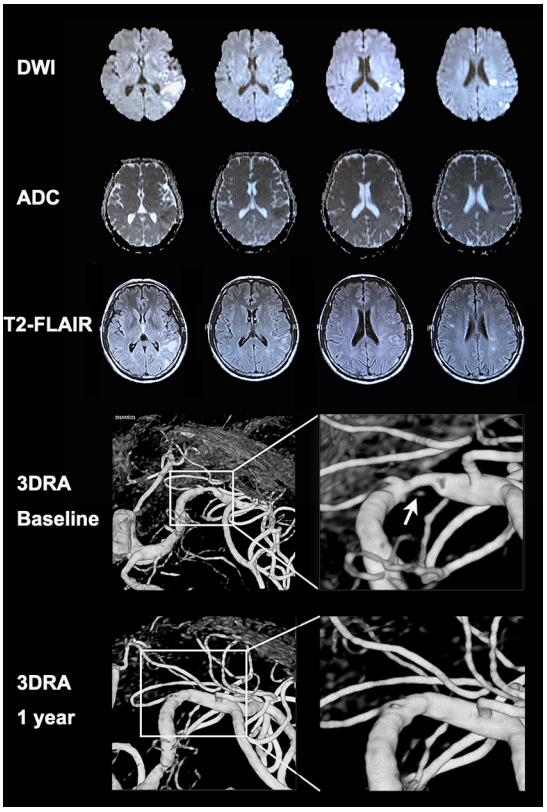


**Figure 3** MRI and 3DRA images of a patient with an ulcerative MCA-M1 plaque and coexisting acute and chronic infarcts in cortical and subcortical regions. A patient with a history of hypertension presented with sudden onset of expressive dysphasia. The MRI exam conducted 1 day after symptom onset showed a cluster of early infarcts (high signal in DWI and low signal in apparent diffusion coefficient maps) at left posterior corona radiata (internal borderzone) and left temporal–parietal cortical and subcortical regions (including the posterior borderzone). There were also older small infarcts (high signal in T2 fluid-attenuated inversion recovery imaging and iso-intensity signal in apparent diffusion coefficient maps) in the same regions. The 3DRA exam conducted 4 weeks after the index stroke showed 80% stenosis of the left MCA-M1 with an ulcer in the plaque surface, that is, contrast appearing beneath the surface outline of the plaque (arrow). The patient received aspirin and clopidogrel treatment for 4 weeks since admission followed by lifelong aspirin treatment, in conjunction with stringent vascular risk factor control. The patient had no recurrent ischaemic stroke within 1 year after the index stroke. A repeated 3DRA exam at 1 year showed healing of the previously ulcerated MCA-M1 plaque. 3DRA, 3-dimensional rotational angiography; DWI, diffusion-weighted imaging; MCA-M1, M1 middle cerebral artery.

complicated intracranial stenting,[2] a careful angiographic evaluation prior to endovascular intervention is warranted in this subgroup.[30] Second, based on the postmortem studies by Fisher and Caplan *et al*, ostial perforator disease favoured atherosclerosis in pathogenesis (ie, BAD), whereas truncal or distal perforator disease might suggest fibrinoid degeneration/lipohyalinosis.[31 32] Therefore, by stringent risk factor control, orifical stenoses of branches/perforators might stand a chance to regress if they were predominantly atherosclerotic or simply extensions of parent large-vessel atheroma.[15 20 33] On the contrary, in the truncal form of perforator disease that entailed fibrinoid degeneration, lipohyalinosis and small haemorrhagic extravasations at the arterial walls, use of intensive antithrombotics should be judicious given the non-atherothrombotic stroke mechanism and probable presence of microbleeds.[31 32]

Our study has the following limitations: first, the median interval from index stroke/TIA onset to 3DRA exam was 23 days. Plaque morphology might evolve during this period under treatments with antiplatelet(s) and statins. Second, vessel opacification in 3DRA was flow-dependent. Therefore, small vessels that were completely occluded, grossly hypoperfused, or of minute calibre (eg, vertebrobasilar perforators) might not be evident in our study, leading to misjudgement of branches/perforators ostium locations. There were cases when orifices of lenticulostriate arteries (rising from the dorsal-superior wall of MCA stem) were invisible even when the MCA plaque was predominantly located over the inferior wall of MCA stem (eg, figure 1G). A plausible explanation could be the Venturi effect, in which the perfusion pressure to the perforators might abruptly drop due to the accelerated jet across the index high-grade stenosis.[34 35] Third, some plaque morphological assessments were susceptible to subjective judgement. We attempted to minimise this potential bias by employing experienced investigators who had moderate to good intrarater and inter-rater reliability in reviewing 3DRA. Further validation of this technique at other centres is warranted. Fourth, 3DRA revealed protruding luminal plaques, while positively remodelled plaques (ie, outward compensatory growth of arterial wall to maintain a constant lumen diameter) required vessel-wall MRI for diagnosis and evaluation.[36 37] Moreover, vessel wall MRI might also provide critical information on plaque components, vessel wall characteristics and the spatial relationship between parent plaque and orifices of penetrating arteries. Coregistration of 3DRA images with vessel wall MRI may provide complementary information in plaque evaluation.[38] As plaque instability is a summation of morphology, plaque components and adverse haemodynamic parameters, a rheology study across the symptomatic ICAD lesions is also crucial to supplement and explain stroke recurrence.

## CONCLUSIONS

3DRA allowed evaluation of morphological traits of intracranial atherosclerotic plaques. Symptomatic high-grade ICAD plaques were mostly eccentric with stenosis most severe over the distal portion. Morphological features differed between smooth, irregular and ulcerative plaques: ulcerative ICAD plaques entailed more vulnerable morphological attributes, adjoining BAD and were associated with a higher incidence of acute-and-chronic infarctions downstream. Further longitudinal studies on the dynamic evolution of plaque morphology, composition and global/focal rheological characteristics will deepen our understanding of stroke mechanisms in the presence of ICAD.

**Author affiliations**
[1]Department of Medicine & Therapeutics, The Chinese University of Hong Kong, Hong Kong SAR, China
[2]Department of Neurology, Beijing Tiantan Hospital, Beijing, China
[3]Department of Medicine and Geriatrics, The United Christian Hospital, Hong Kong SAR, China
[4]Department of Medicine, Pamela Youde Nethersole Eastern Hospital, Hong Kong SAR, China
[5]Department of Medicine, North District Hospital, Hong Kong SAR, China
[6]Department of Medicine and Geriatric, Tuen Mun Hospital, Hong Kong SAR, China
[7]Department of Medicine, The Queen Elizabeth Hospital, Hong Kong SAR, China
[8]Shenzhen Institutes of Advanced Technology Chinese Academy of Sciences, Shenzhen, Guangdong, China
[9]Department of Interventional Neuroradiology, Beijing Tiantan Hospital, Beijing, China
[10]Department of Imaging and Interventional Radiology, The Chinese University of Hong Kong, Hong Kong SAR, China

**Acknowledgements** We would like to thank the study participants and all clinical and research staff who contributed to patient recruitment and care.

**Contributors** TWL, SCHY and XL planned the study, analysed the data, interpreted the findings and wrote the manuscript; LW, XZ, YS and YP contributed to data collection and analyses; HLI, AC, LWCA, FF, SHM, BI, KM, AY-IL, HL, KFH, RL, SHL, MF and WCF contributed to data collection; JL, VM, KSLW, ZM and NM provided critical comments/ revisions of the manuscript. TWL and XL are responsible for the overall content.

**Funding** This work was supported by General Research Fund, Research Grants Council of Hong Kong (Reference numbers 470411, 14138416 and 14106019); National Natural Science Foundation of China/Research Grants Council of Hong Kong Joint Research Scheme (Reference number N_CUHK421/16 & 81661168015); S. H. Ho Foundation (no reference number); Kwok Tak Seng Centre for Stroke Research and Intervention (no reference number); and Young Elite Scientists Sponsorship Program (Reference No. 2017QNRC001), China Association for Science and Technology.

**Disclaimer** The funding source had no role in design and conduct of the study; collection, management, analysis and interpretation of the data; preparation, review or approval of the manuscript; and decision to submit the manuscript for publication.

**Competing interests** None declared.

**Patient consent for publication** Not required.

**Ethics approval** The Joint Chinese University of Hong Kong – New Territories East Cluster Clinical Research Ethics Committee approved the study (Reference No. 2011.021), and each participant provided a written informed consent.

**Provenance and peer review** Not commissioned; externally peer reviewed.

**Data availability statement** Data are available on reasonable request. Anonymised data that support the findings of this study are available from the corresponding author on reasonable request from qualified investigators.



**ORCID iDs**
Thomas W Leung http://orcid.org/0000-0001-8193-0709
Yannie Soo http://orcid.org/0000-0002-3489-3201
Bonaventure Ip http://orcid.org/0000-0002-1619-4992
Alexander Yuk-lun Lau http://orcid.org/0000-0002-5933-9290
Ning Ma http://orcid.org/0000-0002-4909-7048
Simon C H Yu http://orcid.org/0000-0002-8715-5026
Xinyi Leng http://orcid.org/0000-0001-7300-6647

## REFERENCES

1 Holmstedt CA, Turan TN, Chimowitz MI. Atherosclerotic intracranial arterial stenosis: risk factors, diagnosis, and treatment. *Lancet Neurol* 2013;12:1106–14.
2 Derdeyn CP, Chimowitz MI, Lynn MJ, *et al*. Aggressive medical treatment with or without stenting in high-risk patients with intracranial artery stenosis (SAMMPRIS): the final results of a randomised trial. *Lancet* 2014;383:333–41.
3 Wang Y, Zhao X, Liu L, *et al*. Prevalence and outcomes of symptomatic intracranial large artery stenoses and occlusions in China: the Chinese intracranial atherosclerosis (CICAS) study. *Stroke* 2014;45:663–9.
4 Rothwell PM, Gibson R, Warlow CP, *et al*. Interrelation between plaque surface morphology and degree of stenosis on carotid angiograms and the risk of ischemic stroke in patients with symptomatic carotid stenosis. on behalf of the European carotid surgery Trialists' Collaborative group. *Stroke* 2000;31:615–21.
5 Thammongkolchai T, Riaz A, Sundararajan S. Carotid stenosis: role of plaque morphology in recurrent stroke risk. *Stroke* 2017;48:e197–9.
6 Rafailidis V, Chryssogonidis I, Tegos T, *et al*. Imaging of the ulcerated carotid atherosclerotic plaque: a review of the literature. *Insights Imaging* 2017;8:213–25.
7 Fleg JL, Stone GW, Fayad ZA, *et al*. Detection of high-risk atherosclerotic plaque: report of the NHLBI Working group on current status and future directions. *JACC Cardiovasc Imaging* 2012;5:941–55.
8 Stefanadis C, Antoniou C-K, Tsiachris D, *et al*. Coronary atherosclerotic vulnerable plaque: current perspectives. *J Am Heart Assoc* 2017;6:e005543.
9 Vergallo R, Porto I, D'Amario D, *et al*. Coronary atherosclerotic phenotype and plaque healing in patients with recurrent acute coronary syndromes compared with patients with long-term clinical stability: an in vivo optical coherence tomography study. *JAMA Cardiol* 2019;4:321–9.
10 Kim BJ, Kim JS. Ischemic stroke subtype classification: an Asian viewpoint. *J Stroke* 2014;16:8–17.
11 Leng X, Wong KS, Leung TW. The contemporary management of intracranial atherosclerotic disease. *Expert Rev Neurother* 2016;16:701–9.
12 de Weert TT, Cretier S, Groen HC, *et al*. Atherosclerotic plaque surface morphology in the carotid bifurcation assessed with multidetector computed tomography angiography. *Stroke* 2009;40:1334–40.
13 Fisher M. Stroke. geometry is destiny for carotid atherosclerotic plaques. *Nat Rev Neurol* 2012;8:127–9.
14 van Rooij WJ, Sprengers ME, de Gast AN, *et al*. 3D rotational angiography: the new gold standard in the detection of additional intracranial aneurysms. *AJNR Am J Neuroradiol* 2008;29:976–9.
15 Leung TW, Wang L, Soo YOY, *et al*. Evolution of intracranial atherosclerotic disease under modern medical therapy. *Ann Neurol* 2015;77:478–86.
16 Chimowitz MI, Lynn MJ, Derdeyn CP, *et al*. Stenting versus aggressive medical therapy for intracranial arterial stenosis. *N Engl J Med* 2011;365:993–1003.
17 Lovett JK, Gallagher PJ, Hands LJ, *et al*. Histological correlates of carotid plaque surface morphology on lumen contrast imaging. *Circulation* 2004;110:2190–7.
18 Samuels OB, Joseph GJ, Lynn MJ, *et al*. A standardized method for measuring intracranial arterial stenosis. *AJNR Am J Neuroradiol* 2000;21:643–6.
19 Ohara T, Toyoda K, Otsubo R, *et al*. Eccentric stenosis of the carotid artery associated with ipsilateral cerebrovascular events. *AJNR Am J Neuroradiol* 2008;29:1200–3.
20 Caplan LR. Intracranial branch atheromatous disease: a neglected, understudied, and underused concept. *Neurology* 1989;39:1246–50.
21 Nah H-W, Kang D-W, Kwon SU, *et al*. Diversity of single small subcortical infarctions according to infarct location and parent artery disease: analysis of indicators for small vessel disease and atherosclerosis. *Stroke* 2010;41:2822–7.
22 Leng X, Lan L, Ip HL, *et al*. Hemodynamics and stroke risk in intracranial atherosclerotic disease. *Ann Neurol* 2019;85:752–64.
23 Malek AM, Alper SL, Izumo S. Hemodynamic shear stress and its role in atherosclerosis. *JAMA* 1999;282:2035–42.
24 Li X, Yang Q, Wang Z, *et al*. Shear stress in atherosclerotic plaque determination. *DNA Cell Biol* 2014;33:830–8.
25 Feng X, Chan KL, Lan L, *et al*. Stroke mechanisms in symptomatic intracranial atherosclerotic disease: classification and clinical implications. *Stroke* 2019;50:2692–9.
26 Wong KSL, Chen C, Fu J, *et al*. Clopidogrel plus aspirin versus aspirin alone for reducing embolisation in patients with acute symptomatic cerebral or carotid artery stenosis (clair study): a randomised, open-label, blinded-endpoint trial. *Lancet Neurol* 2010;9:489–97.
27 Wong KSL, Wang Y, Leng X, *et al*. Early dual versus mono antiplatelet therapy for acute non-cardioembolic ischemic stroke or transient ischemic attack: an updated systematic review and meta-analysis. *Circulation* 2013;128:1656–66.
28 Lin W, Xiong L, Han J, *et al*. External counterpulsation augments blood pressure and cerebral flow velocities in ischemic stroke patients with cerebral intracranial large artery occlusive disease. *Stroke* 2012;43:3007–11.
29 Petrone L, Nannoni S, Del Bene A, *et al*. Branch atheromatous disease: a clinically meaningful, yet unproven concept. *Cerebrovasc Dis* 2016;41:87–95.
30 Leung TW, Yu SCH, Lam WWM, *et al*. Would self-expanding stent occlude middle cerebral artery perforators? *Stroke* 2009;40:1910–2.
31 Fisher CM. The arterial lesions underlying lacunes. *Acta Neuropathol* 1968;12:1–15.
32 Caplan LR. Lacunar infarction and small vessel disease: pathology and pathophysiology. *J Stroke* 2015;17:2–6.
33 Mok V, Kim JS. Prevention and management of cerebral small vessel disease. *J Stroke* 2015;17:111–22.
34 Soustiel JF, Levy E, Bibi R, *et al*. Hemodynamic consequences of cerebral vasospasm on perforating arteries: a phantom model study. *Stroke* 2001;32:629–35.
35 Ritter MA, Ringelstein EB. The Venturi effect and cerebrovascular ultrasound. *Cerebrovasc Dis* 2002;14:98–104.
36 Xu W-H, Li M-L, Gao S, *et al*. Plaque distribution of stenotic middle cerebral artery and its clinical relevance. *Stroke* 2011;42:2957–9.
37 Bodle JD, Feldmann E, Swartz RH, *et al*. High-Resolution magnetic resonance imaging: an emerging tool for evaluating intracranial arterial disease. *Stroke* 2013;44:287–92.
38 Guan M, Lin Jia'xing, Huang Sheng'ming, *et al*. High-Degree Middle Cerebral Artery Stenosis : Can Advanced 3D DSA-MRI Fusion Imaging Better Illustrate Plaques and Perforators? *Clin Neuroradiol* 2020;2:s00062-020-00927-w.